JOURNAL OF MATERIALS SCIENCE 31 (1996) 4603–4608

The effect of elevated temperature and silicon addition on a cobalt-based wear resistant superalloy

A. OSMA, E. S. KAYALI, M. L. ÖVEÇOĞLU
Metallurgical Engineering Department, Istanbul Technical University, Maslak 80626, Istanbul, Turkey

The effects of an elevated temperature and a 5 wt% silicon addition on the resultant microstructure and inherent phases of Stellite 6 were investigated by using room and high temperature optical microscopy, X-ray diffraction, scanning electron microscopy (SEM) and also bulk hardness and microhardness measurements. It has been observed that exposing Stellite 6 to heat treatments at 1000 °C results in a characteristic textured structure and coarsening of interdendritic regions due to bulk diffusion. In addition, both dendritic and interdendritic hardness values increase due to texture formation and increased amounts of carbide and intermetallic phases, respectively. On the other hand, silicon addition to Stellite 6 causes the transformation of the original spongy dendritic microstructure in as-cast Stellite 6 to a eutectic dendritic and skeleton interdendritic structure. Also, when silicon added Stellite 6 was heat treated at 1000 °C, particulates emanating from the interdendritic skeleton become irregularly dispersed in the dendritic region. In addition, similarly to Stellite 6; a high temperature heat treatment results in an increase in hardness values of silicon added Stellite 6 due to the presence of an Co_2Si intermetallic phase.

1. Introduction

Cobalt-base superalloys are used in wear-related engineering applications at temperature ranges of 650–1100 °C [1–3]. Stellite is a commercial cobalt-base wear resistant superalloy that was originally developed with a cobalt–chromium composition which has been modified by the addition of elements such as tungsten, molybdenum, silicon and iron [3–5]. The mechanical properties of cobalt-base superalloys strongly depend on the presence of precipitated phases such as carbides, intermetallics and also their microstructures.

Although pure cobalt has a phase transformation from a low-tempertaure hexagonal-closed packed (ε-h.c.p.) structure to a high-temperature face-centered cubic (γ-f.c.c.) structure at 417 °C [4–8], most cobalt-base alloys are characterized by a face-centered cubic (γ-f.c.c.) matrix containing second phases [8–11]. These second phases are various carbides and different intermetallic phases that are geometrically closed-packed phases (g.c.p.) with a A_3B form such as γ-(Ni, Co)$_3$(Al, Ti), η-Ni_3Ti and topologically closed-packed phases (t.c.p.) which can be seen in cobalt-base alloys such as σ-(Co, Ni)(Cr, Mo, W), μ-Co_7W_6, Laves (A_2B) and π-(Co, Ni, Cr, W)C [9–12]. The study of the Co–Cr–C phase diagram shows that some carbides of cobalt are formed in cobalt-base alloys [6, 13]. Atamert and Bhadeshia [14] and Antony [3] have observed M_7C_3 and M_6C carbides in Stellite alloys. However, Boultbee and Schofield [15] have described a M_7C_3 carbide in Stellite 1 grade and $M_{23}C_6$ carbide in Stellite 6 grade. Rothman *et al.* [9] have also reported $M_{23}C_6$, Cr_7C_3 and M_6C types of carbides in Stellite 6.

The aim of this investigation is to observe the effects of elevated temperature exposure and silicon addition on as-cast Stellite 6 alloy. For this purpose, analytical experimental techniques such as room and, high temperature optical microscopy, X-ray diffraction, scanning electron microscopy and also bulk hardness and microhardness measurements were utilized.

2. Experimental procedure

The Stellite 6 and 5 wt% Si added Stellite used in this investigation were received from a group working on hardfacing alloys at Cambridge University [14]. Both alloys were melted in an arc furnace and were sand cast. The nominal chemical compositions of the alloys used in this investigation were respectively, Co–28Cr–4W–1C(wt%) and Co–28Cr–4W–1C–5Si (wt%). Characterization studies were conducted by using room and high temperature optical microscopy, scanning electron microscopy (SEM), X-ray diffraction, bulk hardness and microhardness testing on specimens prepared from both as-cast and heat-treated samples.

In order to determine the microstructure of these alloys, samples for metallographic examination were studied in the standard manner. Metallographic

0022–2461

specimens were prepared by mechanical polishing and chemical etching in a 5 ml H_2O_2 + 100 ml HCl + 5 ml H_2O solution. The microstructure of the alloys were observed *in-situ* using a high temperature Leitz optical microscope between 25–1000 °C in order to determine microstructural changes and phase transformation. In addition, heat-treatments simulating the high temperature microscopy conditions were performed to produce X-ray diffraction samples for bulk phase analyses. These, heat-treatments were at 1000 °C for 30 min on as-cast Stellite 6 and silicon added Stellite 6 followed by an air cool. Data were taken on these samples in addition to as cast material. The secondary electron imaging (SEI) mode of Jeol JSM-T330 scanning electron microscope equipped as the Tracor TN-5500 energy dispersive spectrometer (EDX) was used to examine changes in microstructure and chemical compositions of both as-cast and heat-treated samples. A Vickers diamond indentor with varying loads was used on both as-cast and heat-treated samples to determine bulk hardness and microhardness of different microstructural regions.

3. Results and discussion

Figs 1 and 2 show the microstructure of as-cast and heat-treated at 1000 °C for 30 min under vaccum Stellite 6 in a hot-stage optical microscope, respectively. Fig. 1 shows a typical coarse dendritic microstructure with narrow interdendritic regions obtained as a result of sand-casting. When Stellite 6 was exposed to high temperatures, a structure with coarser interdendritic

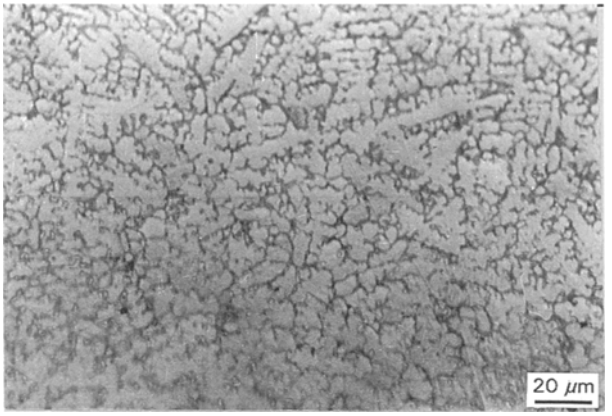

Figure 1 Optical micrograph of as-cast Stellite 6.

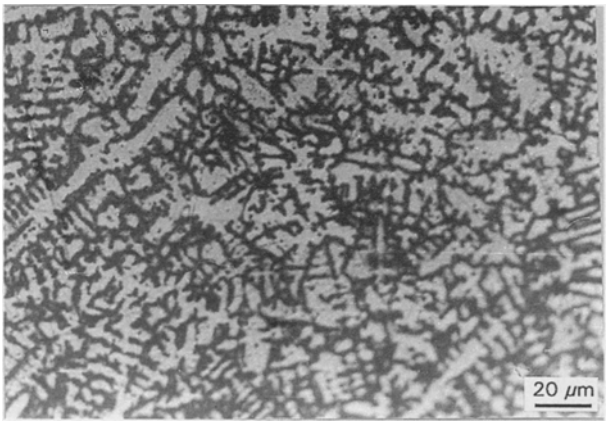

Figure 2 Optical micrograph of as-cast Stellite 6 heated to 1000 °C under vacuum in a hot-stage microscope.

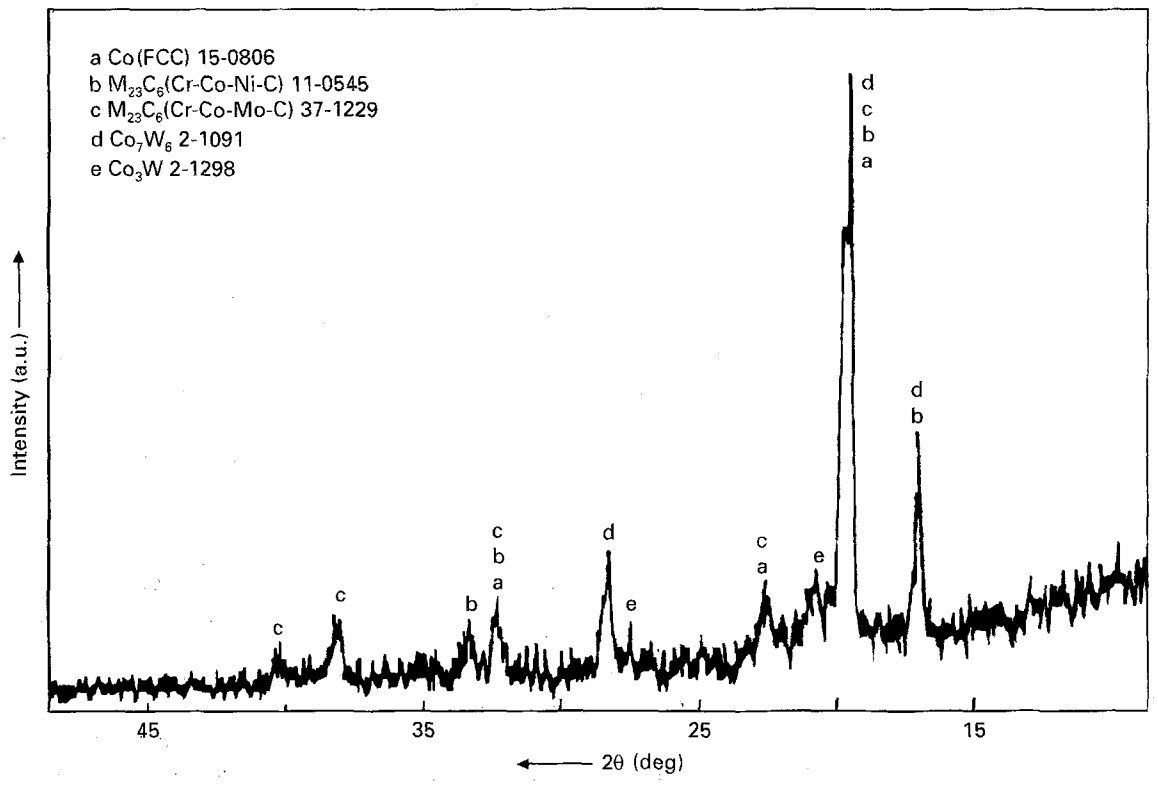

Figure 3 X-ray diffraction data of as-cast Stellite 6. The phases identified from JCPDS powder diffraction files are indicated.

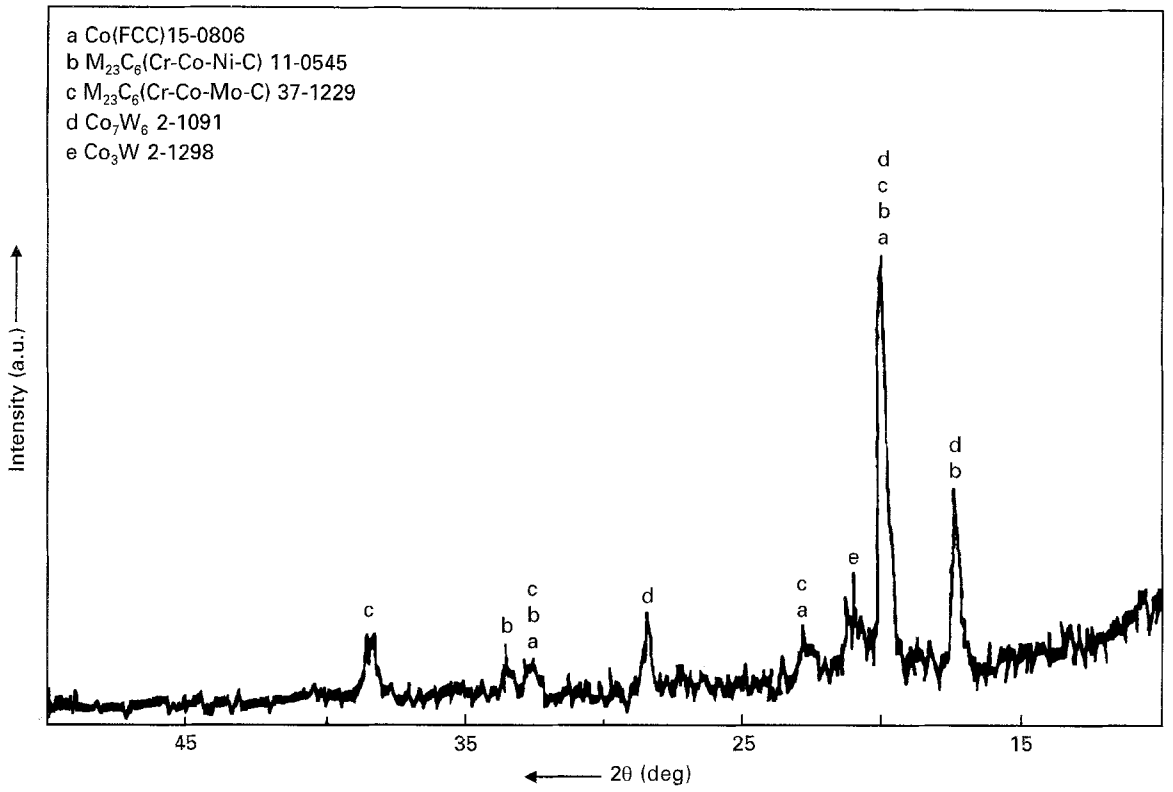

Figure 4 X-ray diffraction data of as-cast Stellite 6 heated to 1000 °C and then cooled in the air. The phases identified from JCPDS powder diffraction files are indicated.

regions and finer dendrites than those for the as-cast sample formed, as seen in Fig. 2. This is probably due to bulk diffusion taking place from dendrites to interdendritic regions. No significant changes in the microstructure of silicon added Stellite 6 were observed under vacuum in the hot-stage optical microscope.

X-ray diffraction patterns were taken from both as-cast and heat-treated samples. Figs 3 and 4 show the X-ray data of as-cast and heat-treated Stellite 6, respectively. From the X-ray patterns (γ-f.c.c.) Co, $M_{23}C_6$, Co_7W_6, Co_3W phases were detected in the as-cast and heat-treated Stellite 6 which is in agreement with other work on this system [9–12]. Figs 5 and 6 show the X-ray data of as-cast and heat-treated silicon added Stellite 6, respectively. These patterns reveal the presence of the (γ-f.c.c.)Co, $M_{23}C_6$ and also a Co_2Si phase which had not been reported in previous studies [10, 11, 16]. On the basis of these X-ray diffraction experiments it appears that the addition of silicon to Stellite 6 favours the formation of a Co_2Si phase over the cobalt–tungsten intermetallic phases Co_7W_6 and Co_3W observed in Stellite 6. Co_2Si forms as a result of cobalt affinity for silicon due to a larger disparity in the periodic table between cobalt and silicon than that between cobalt and tungsten. In other words, with the addition of silicon to Stellite 6 retained cobalt is scavenged by silicon.

SEM micrographs and pertinent EDX results of as-cast and heat-treated Stellite 6 are given in Figs 7 and 8, respectively. It is believed that the spongy appearance of the dendritic regions is a result of (γ-f.c.c.) Co-rich solid solution and uniformly distributed intermetallic phase particles. Two phases distinguished as darker and lighter grey colours can be depicted in interdendritic regions in Fig. 7(a and b). Based on the EDX analysis, the light grey region is rich in chromium which exists possibly in the form of $M_{23}C_6$. Considering both the EDX and X-ray diffraction data together, the formation of complex $M_{23}C_6$ carbides is expected in the interdendritic regions. Textured structure in the dendritic and a characteristic two phase structure in the interdendritic regions are observed in the heat-treated sample (Fig. 8(a and b)). Incoherent intermetallic phases which exist as Widmanstatten plates become oriented along the habit planes of the matrix phase forming the textured structure in the dendritic regions. Evaluation of EDX analyses given in Figs 7a and 8a indicates that the cobalt and chromium contents of the dendrites remain unchanged by heat treatment at elevated temperatures. However, as seen in Fig. 8b, a high temperature promotes bulk diffusion of tungsten from the dendrites to the interdendritic regions forming carbide phases and/or intermetallic phases (Co_7W_6 and Co_3W) within the interdendritic regions. Furthermore, the interdendritic regions in the heat-treated sample are comprised of black lamellar and grey coloured zones. Based on this observation and EDX analysis (Fig. 8b), (γ-f.c.c.) Co solid solution and complex $M_{23}C_6$ carbide phases coexist in the interdendritic regions [6, 10, 11].

The effect of silicon addition on the microstructure of as-cast and heat-treated Stellite 6 are given in Figs 9 and 10, respectively. Silicon addition to Stellite 6 promotes the eutectic structure with dark dendritic and

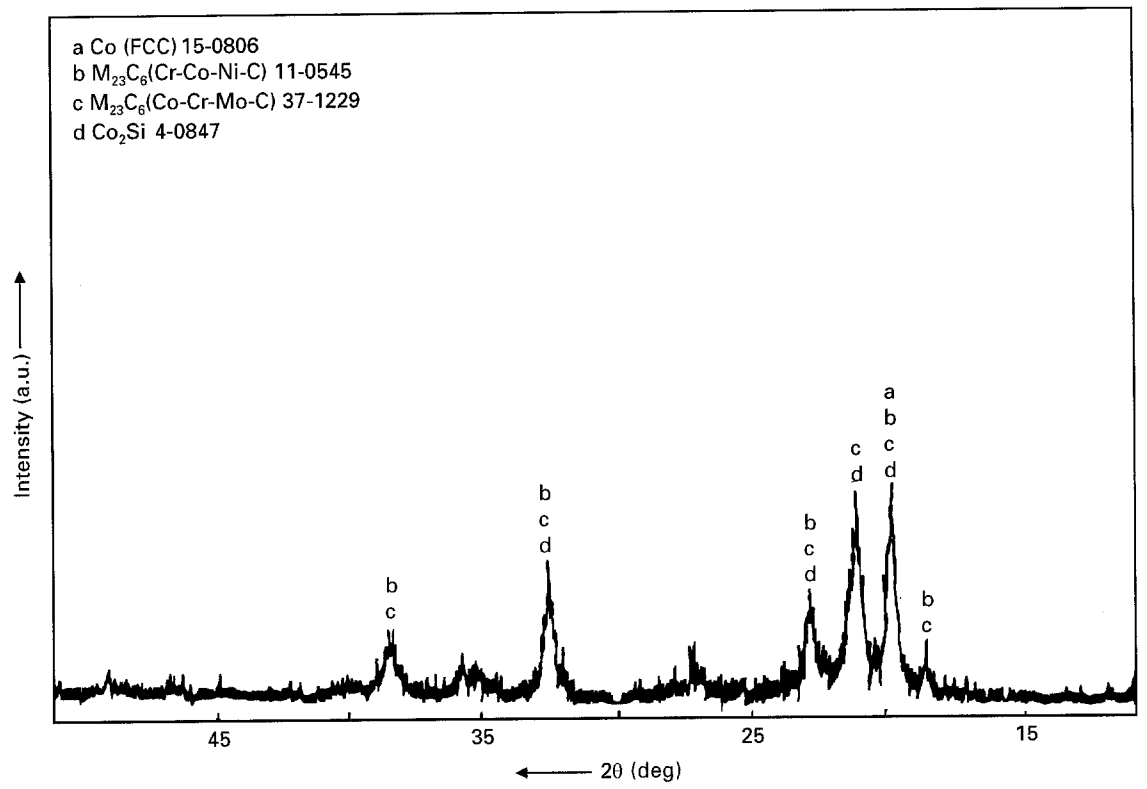

Figure 5 X-ray diffraction data of as-cast silicon added Stellite 6. The phases identified from JCPDS powder diffraction files are indicated.

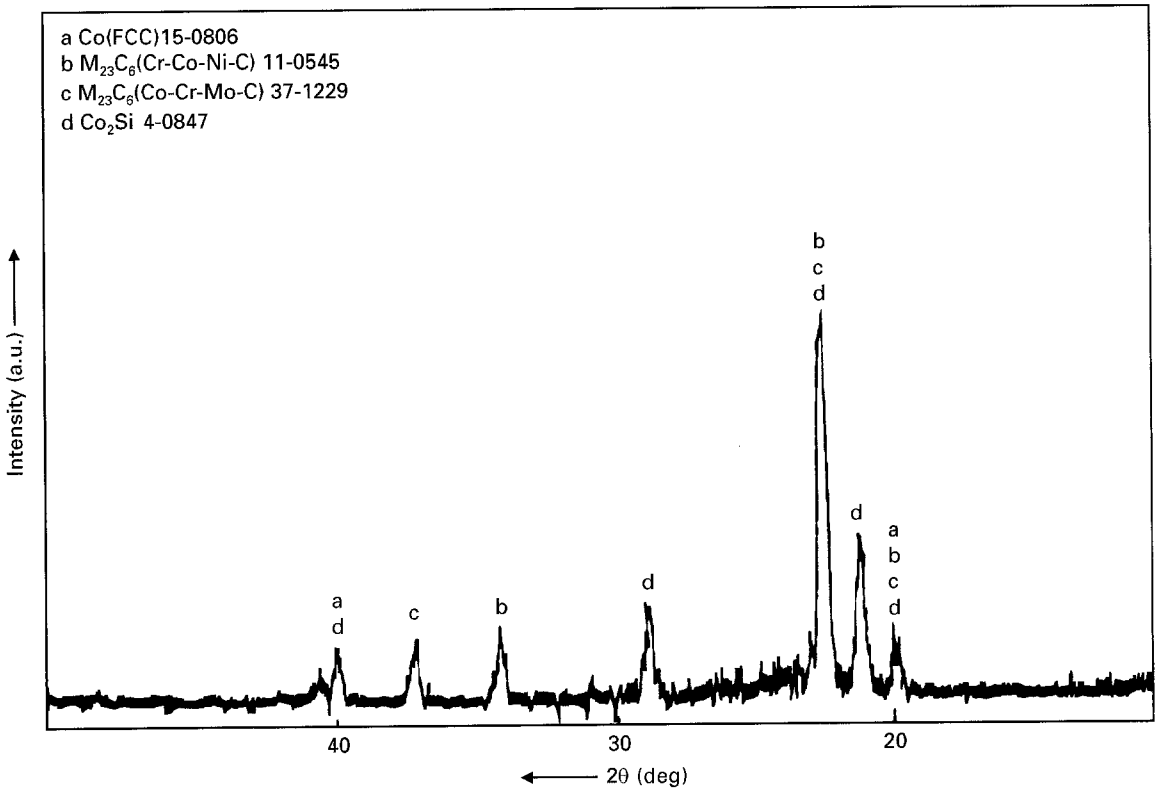

Figure 6 X-ray diffraction data of as-cast silicon added Stellite 6 heated to 1000 °C and then cooled in the air. The phases identified from JCPDS powder diffraction files are indicated.

white skeleton interdendritic regions. Based on the EDX analysis and X-ray diffraction data together, it can be stated that the dark coloured dendritic regions are a cobalt-rich, (γ-f.c.c.) Co solid solution matrix and that the white coloured skeleton interdendritic regions are rich in a chromium-containing complex $M_{23}C_6$ carbides and Co_2Si intermetallic phases. As seen in Fig. 10, when silicon containing Stellite 6 was

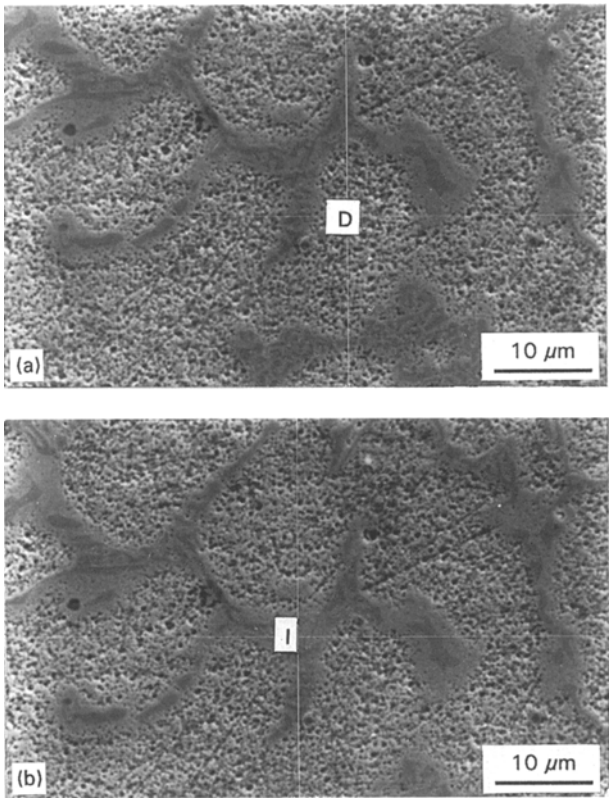

Figure 7 SEM micrographs and EDX analyses of as-cast Stellite 6. a) EDX analysis taken from dendritic region (D: 61.78 Co–29.93Cr–4.68 W(wt %)), b) EDX analysis taken from interdendritic region (I: 22.68Co–70.81Cr–4.01W(wt %)).

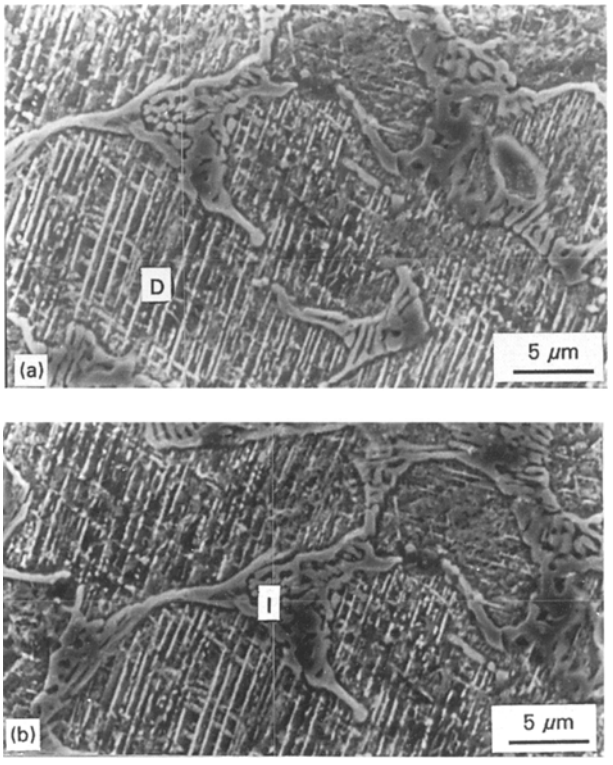

Figure 8 SEM micrographs and EDX analyses of as-cast Stellite 6 heated to 1000 °C and cooled in air. a) EDX analysis taken from dendritic region (D: 62.44Co–30.42Cr–3.13W(wt %)), b) EDX analysis taken from interdendritic region (I: 39.65 Co–50.89Cr–6.4W(wt %)).

heated to 1000 °C, particulates emanating from the interdendritic skeleton became irregularly dispersed in the dendritic region. On the other hand, the chemical compositions of both interdendritic and dendritic

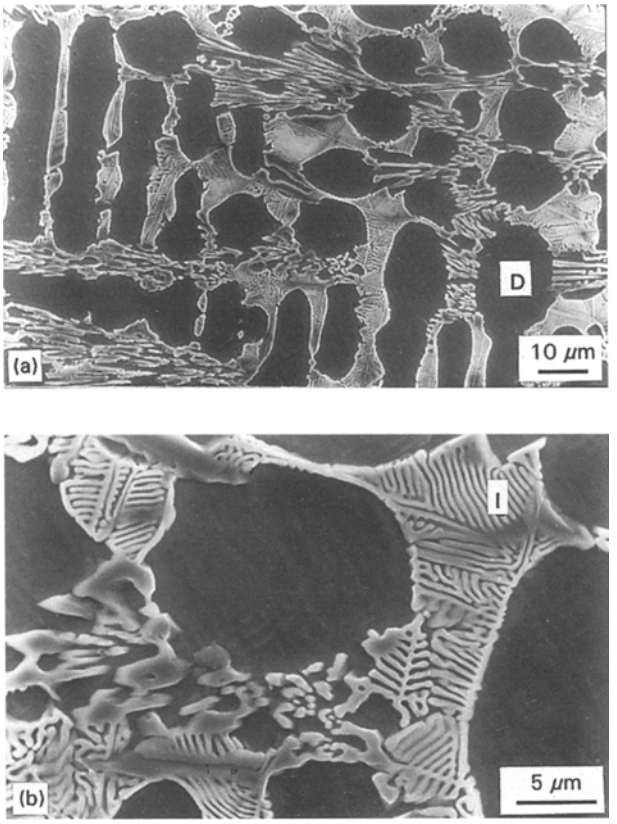

Figure 9 SEM micrographs and EDX analyses of as-cast silicon added Stellite 6. a) EDX analysis taken from dendritic region (D: 64.69Co–25.99Cr–2.98W–6.34Si(wt %)), b) EDX analysis taken from interdendritic region (I: 45.03Co–33.60Cr–10.06W–11.31Si(wt %)).

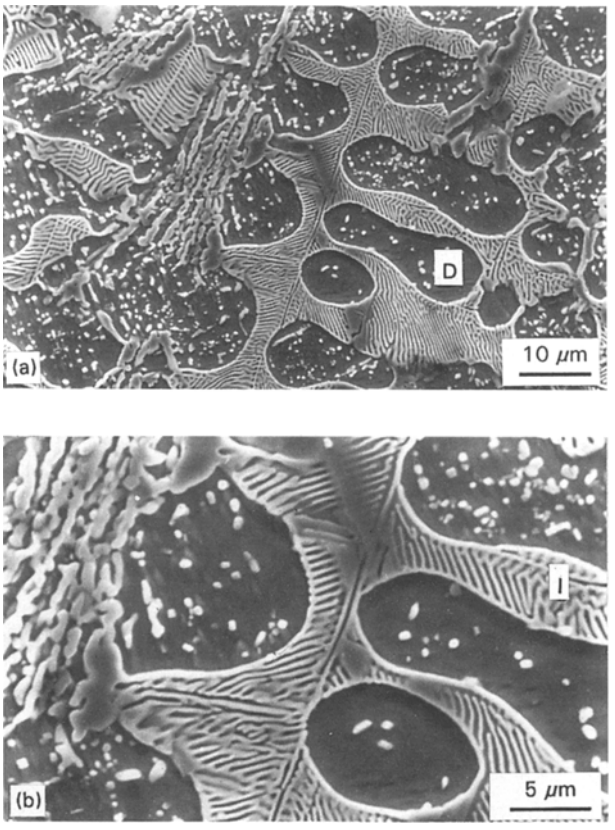

Figure 10 SEM micrographs and EDX analyses of as-cast silicon added Stellite 6 heated to 1000 °C and cooled in air. a) EDX analysis taken from dendritic region (D: 65.62Co–26.35Cr–2.24W–5.79Si(wt %)), b) EDX analysis taken from interdendritic region (I: 41.40Co–31.68Cr–10.29W–16.63Si(wt %)).

TABLE I Hardness measurements of as-cast and heat-treated Stellite 6

Regions	Hardness (H_v/kg mm^{-2})	
	As-cast sample	Heat-treated sample
Bulk	514	605
Dendritic	506	543
Interdendritic	585	705

TABLE II Hardness measurements of as-cast and heat-treated silicon added Stellite 6

Regions	Hardness (H_v/kg mm^{-2})	
	As-cast sample	Heat-treated sample
Bulk	643	785
Dendritic	627	717
Interdendritic	800	919

regions of silicon containing Stellite 6 remain almost unchanged after elevated temperature exposure. The effect of silicon addition to Stellite 6 is to transform the spongy dendritic microstructure seen in the original as-cast Stellite 6 to an eutectic microstructure. After heat-treatment at 1000 °C, textured Widmanstatten plates form in Stellite 6 whereas eutectic interdendritic and dendritic regions are retained in addition to fragmented particulates of interdendritic composition in silicon added Stellite 6.

As tabulated in Table I, bulk hardness and microhardness measurements performed on both as-cast and heat-treated samples indicate a subsequent rise in bulk hardness, dendritic and interdendritic hardness values due to elevated temperature exposure. The increase of overall bulk hardness is about 17%. An increase in interdendritic hardness values due to elevated temperature exposure might be related to the relative increase in the population of carbides and/or intermetallic phases. Also, the textured structure of dendritic regions inherent in the heat-treated sample contributes to the relative increase in microhardness values.

Table II shows the hardness values of silicon added Stellite 6 taken from the bulk, dendritic and interdendritic regions. Similarly to Stellite 6, high temperature exposure results in an increase in hardness values of silicon added Stellite 6. Furthermore, comparing the values given in Tables I and II for both as-cast and heat-treated samples; it can be stated that silicon addition causes substantial increases in the hardness values. It is believed that the Co_2Si intermetallic phase observed in silicon added Stellite 6 contributes to hardness to a greater extent than does the cobalt-tungsten intermetallic phases observed in Stellite 6.

4. Summary

On the basis of the microstructural observations and experimental data, the following conclusions can be drawn:

1) High temperature exposure of Stellite 6 promotes the coarsening of interdendritic regions and bulk diffusion of tungsten from dendritic to interdendritic regions and contributes to the increase of cobalt–tungsten intermetallic phases in the interdendritic regions.

2) A textured structure which exists as Widmanstatten plates, containing incoherent intermetallic phases, is developed in the dendritic regions of Stellite 6 after heating at 1000 °C followed by cooling in air. On the other hand, silicon addition causes the transformation of the spongy dendritic microstructure into a well-defined eutectic microstructure for as-cast samples where a similar microstructure exist with interdendritic fragments after high temperature exposure.

3) The same phases previously reported in the literature such as (γ-f.c.c.) Co, ($M_{23}C_6$), Co_7W_6, Co_3W were detected in as-cast and heat-treated Stellite 6. The X-ray diffraction data of silicon added Stellite 6 in as-cast and heat-treated samples show some of the same phases, namely, (γ-f.c.c.) Co, $M_{23}C_6$ but in addition Co_2Si was detected. Silicon addition to Stellite 6 favours the formation of the Co_2Si phase in both as-cast and heat-treated samples which contributes to higher hardness values than those obtained for Stellite 6 alloy.

4) High temperature exposure of both Stellite 6 and silicon added Stellite 6 causes an increase in overall hardness values.

References

1. Cobalt Monograph Edited by Center D'Information du Cobalt, 35, Rue Des Colonies, Brussels, Belgium (1960) p. 362.
2. Short Reports, *Mat. Engng.* (Cleveland), 106(9), (Sept. 1989) p. 39.
3. K. C. ANTONY, *J. of Metals* **35** (1983) 52.
4. W. BETTERIDGE, in "Cobalt and Its Alloys" (Ellis Horwood Ltd., England, 1982) p. 61, 119.
5. Metals Handbook, Vol. 2, 10th Edn (ASM, Metals Park, OH, 1990) p. 446.
6. C. R. BROOKS, in "Heat Treatment, Structure and Properties of Nonferrous Alloys" (ASM, Metals Park, OH, 1982) p. 229.
7. Metals Handbook, Vol. 7, 8th Edn (ASM Metals Park, OH, 1972) p. 187.
8. Metals Handbook, Vol. 9, 9th Edn (ASM Metals Park, OH, 1985) p. 334.
9. M. F. ROTHMAN, R. D. ZORDAN and D. R. MUZYKA, in "ASM Conference on Refractory Alloying Elements in Superalloys-Effects and Availability", Rio de Janerio, Brazil, 6–13 April 1984 (ASM, Metals Park, OH, 1984) pp. 102–4.
10. C. T. SIMS, in "The Superalloys", edited by C. T. Sims and W. C. Hagel (John Wiley and Sons, USA, 1972) pp. 146–61.
11. A. M. BELTRAN, in "Superalloys II" edited by C. T. Sims, N. S. Stoloff and W. C. Hagel (John Wiley and Sons, USA, 1987) pp. 143–51.
12. Z. OPIEKUN, *J. Mater. Sci.* **26** (1991) 3386.
13. Metals Handbook, Vol. 8, 8th Edn (ASM, Metal Park, OH, 1973) p. 401.
14. S. ATAMERT and H. K. D. H. BHADESHIA, *Med. Trans. A.* **20A** (1989) 1037.
15. E. F. BOULTBEE and G. A. SCHOFIELD, in "Typical Microstructure of Cast Metals" (The Institute of British Foundrymen, Birmingham, 1981) pp. 236–37.
16. R. W. G. WYCKOFF, in "Crystal Structure", Vol. 1, 2nd Edn (John Wiley and Sons Inc., USA, 1965) p. 305

Recieved 22 February 1995
and accepted 15 January 1996